Observation of Collective Superstrong Coupling of Cold Atoms to a 30-m Long Optical Resonator

Aisling Johnson,[1] Martin Blaha,[1,3] Alexander E. Ulanov,[2] Arno Rauschenbeutel,[1,3] Philipp Schneeweiss,[1,3] and Jürgen Volz[1,3,*]

[1]*Vienna Center for Quantum Science and Technology, TU Wien-Atominstitut, Stadionallee 2, 1020 Vienna, Austria*
[2]*Russian Quantum Center, 100 Novaya Street, Skolkovo, Moscow 143025, Russia*
[3]*Department of Physics, Humboldt-Universität zu Berlin, Newtonstr. 15, 12489 Berlin, Germany*

(Received 15 May 2019; revised manuscript received 12 August 2019; published 11 December 2019)

We report on the observation of collective superstrong coupling of a small ensemble of atoms interacting with the field of a 30-m long fiber resonator containing a nanofiber section. The collective light-matter coupling strength exceeds the free-spectral range and the atoms couple to consecutive longitudinal resonator modes. The measured transmission spectra of the coupled atom-resonator system provide evidence of this regime, realized with a few hundred atoms with an intrinsic single-atom cooperativity of 0.13. These results are the starting point for studies in a new setting of light-matter interaction, with strong quantum nonlinearities and a new type of dynamics.

DOI: 10.1103/PhysRevLett.123.243602

In recent years, the control of light-matter interaction at the fundamental quantum-mechanical level has already proven successful, e.g., for the implementation of quantum metrology, quantum simulation, quantum communication, and information processing. A milestone in this endeavor was the realization of strong coupling between single quantum emitters and single photons in cavity QED [1]; in this regime, the coherent emitter-photon dynamics is faster than all incoherent decay rates of the system. In ensuing experiments, this achievement led to a variety of applications [2] such as controlled quantum state transfer [3–5], backaction-free state detection [6], or the implementation of new quantum protocols [7–9].

Interfacing the resonator mode simultaneously with many identical quantum emitters such as neutral atoms not only allowed extremely large collective light-matter coupling strengths to be reached [10], but also initiated new approaches for quantum devices. These include single-photon transistors [11], new methods for the generation of collective mesoscopic quantum states [12,13] and real-time observation of optical photons [14]. Furthermore, in such systems, the resonator mode can be employed to provide an infinite-range interaction between the different atomic qubits, a key ingredient for the study of the quantum dynamics of collective light-matter systems [15–18]. Moving beyond coupling with a single electromagnetic mode, new experimental platforms where atoms couple with a number of degenerate, higher-order transverse resonator modes, are under development [19–21]. These could be employed, for instance, for photonic quantum information processing [22].

A largely unexplored regime of cavity QED is reached when a single emitter or an ensemble of emitters interacts strongly with several nondegenerate, longitudinal modes of a long cavity. This scenario bridges the gap between two archetypical regimes of light-matter interaction: the strong coupling of emitters to a single resonantly enhanced field mode, giving rise to, e.g., vacuum-induced Rabi oscillations [23], and the coupling of emitters to a single spatial mode with a continuous spectrum, enabling applications such as efficient single-photon sources [24]. In this regime of so-called superstrong coupling [25], the emitter-resonator coupling strength exceeds the free-spectral range (FSR) of the resonator as well as the single-emitter decay rate. Previous investigations in the microwave and acoustic domains [26,27] have recently put this novel regime in the spotlight.

Here, we realize superstrong coupling (SSC) with a small ensemble of atoms that is coupled to a 30-m long optical fiber ring resonator. In the transmission spectrum, several longitudinal cavity resonances are significantly modified and collective coupling strengths largely exceeding the FSR are observed. We determine the number of coupled atoms by analyzing the second-order correlation function of fluorescence light scattered into the fiber ring. Remarkably, SSC is reached in our experiment with as little as 200 atoms. At the same time, we infer an intrinsic single-atom cooperativity of 0.13, meaning that the system's dynamics depends on a quantized degree of freedom as its response will be nonlinear at the level of a few photons. This sets our work apart from more conventional situations in, e.g., laser physics, where the dispersion of a macroscopic medium inside the resonator can exceed the FSR.

Our experiment relies on four key aspects [28]. First, the light field in the resonator and the atoms are coupled via the evanescent field surrounding the nanofiber-waist of a

tapered optical fiber (TOF) [29,30]. The strong transverse confinement of the nanofiber-guided light gives rise to a large single-pass atom–field coupling strength. Second, thanks to the low transmission losses, a TOF can be turned into an optical resonator. Indeed, strong atom-light coupling was demonstrated for TOF-based Fabry-Perot and ring resonators [31,32]. Third, our resonator consists of a ~30-m long fiber ring, whose FSR is as small as $\nu_{\mathrm{FSR}} = 7.1$ MHz, 8 orders of magnitude smaller than the carrier frequency of the optical field. In this geometry, the single-atom cooperativity $C_1 = g_1^2/2(\kappa_0 + \kappa_{\mathrm{ext}})\gamma$ (κ_0 being the intrinsic cavity loss rate, κ_{ext} the in- and out-coupling rate, γ the spontaneous decay rate of a single atom, and g_1 the single-atom–single-photon coupling strength) is independent of resonator length as long as the fiber propagation losses can be neglected compared to the overall round-trip losses [28], mostly dominated by length-independent contributions. In the Supplemental Material [33], we provide a detailed description of the sources of loss to justify this claim. Thus, the FSR of the resonator can be decreased without affecting C_1. Finally, to further enhance the coupling, we use a small ensemble of N laser-cooled atoms interacting with the resonator with a collective strength $g_N = \sqrt{N} g_1$.

The experimental sequence alternates between two phases: a preparation phase, during which the resonator frequency is actively stabilized and a cloud of cold Cs is prepared around the nanofiber by means of a magneto-optical trap (MOT), and a probing phase, where the locking is intermittently interrupted. The resonator frequency is locked to the probe laser using polarization spectroscopy with feedback onto a piezoelectric actuator (see Supplemental Material, [33]) [36,37]. In our setup, see Fig. 1, a variable fiber beam splitter (FBS) allows us to control the coupling rate of light into and out of the resonator [28]. We use two settings of this FBS: For the first setting, the coupling rate is chosen such that the on-resonance transmission through the coupling fiber is minimized for the bare resonator. We refer to this critical coupling configuration as the fiber loop being closed. All later measurements on SSC are performed under this condition. For the second setting, the light only takes one round-trip in the resonator. We also refer to this fully overcoupled regime as the fiber loop being open. This second setting allows us to deduce the single-pass on-resonance optical depth (OD) of our atomic sample measured through the waveguide.

We measure transmission spectra of the coupled atom-resonator system with open and closed fiber loop. The probing phase consists of two measurement intervals of 1-ms duration, a first interval with atoms and a reference interval without atoms. The probe power is chosen such that the mean intracavity photon number is < 1. Within each interval, the probe field's frequency is swept over 40 MHz (about five FSRs) with an acousto-optical

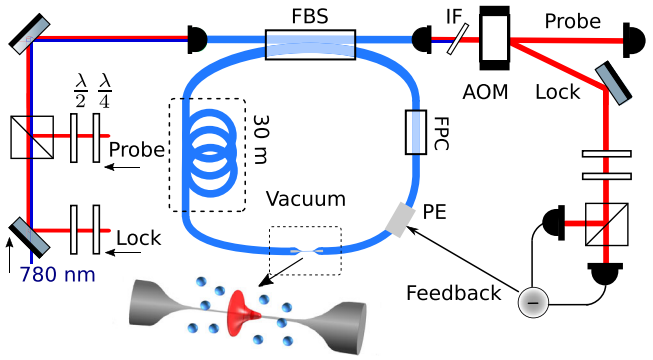

FIG. 1. Sketch of the 30-m long fiber-ring resonator with a nanofiber section for coupling atoms to the resonator mode via its evanescent field part. The probe light (optical power: 1 pW, wavelength: 852 nm, resonant with the $D2$ cycling transition of cesium), the lock light (10 μW), and the heating laser light (1 mW, wavelength: 780 nm) are combined, fiber coupled, and sent into a variable fiber beam splitter (FBS) which couples light into and out of the resonator. The polarizations of the probe and lock light are independently controlled by wave plates and the eigenpolarizations of the resonator are set using fiber polarization controllers (FPC). The resonator is placed inside an acoustically and thermally insulating box, except for the section fed into the vacuum chamber, which contains the nanofiber waist of the TOF (diameter: 400 nm, length: 1 cm). A cloud of laser-cooled atoms is overlapped with the waist. During the preparation phase, the lock light is directed towards a polarization detection setup using an acousto-optical modulator (AOM). The generated lock signal is fed back onto a piezoelectric element (PE) which stretches the fiber to compensate for external perturbations. During the probing phase, the resonator output is then redirected onto a single-photon counting module. An interference filter (IF) removes the 780-nm heating light prior to the detection.

modulator. The transmission spectra are acquired using a single-photon counting module. Figures 2(a) and 2(b) present experimental transmission spectra with the fiber loop being open and closed, respectively. With the open fiber loop (a), the transmission is inhibited by the atomic cloud over a frequency range of more than 10 MHz. The fit shown in red yields an on-resonance optical depth of OD = 12.7. For the closed fiber loop (b), without atoms, the transmission spectrum shows the equidistant resonances of the empty cavity, see gray line. For the coupled atom-resonator system, the measured spectrum (blue line) qualitatively differs from both the empty resonator and the single-pass transmission spectrum of the atoms. In particular, the central resonance is split and higher-order resonances are shifted outwards. The theoretical prediction (red line, see [33]) only contains a residual atom-resonator detuning, $\Delta_{\mathrm{at}} = \omega_{\mathrm{at}} - \omega_{\mathrm{res}}$, as a free fit parameter. The latter is found to be $\Delta_{\mathrm{at}}/2\pi = 150$ kHz. The underlying collective coupling strength, $g_N/2\pi = 8.7$ MHz, was deduced from the OD measured in Fig. 2(a). The very good agreement between theory and measurement, for g_N well in excess of the FSR, clearly reveals that our system

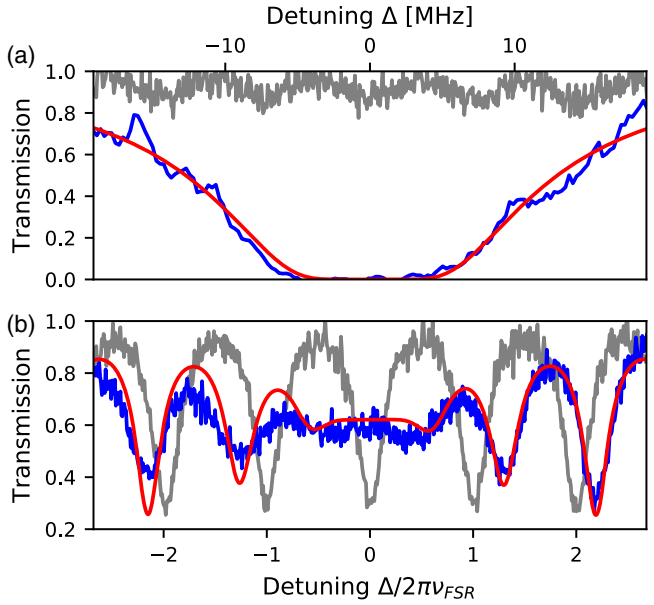

FIG. 2. (a) Measured single-pass transmission spectrum of a MOT cloud acquired through the TOF with the fiber loop being open (blue line). The atomic cloud is optically dense in a frequency range of about ± 10 MHz around the atomic resonance with a single-pass on-resonance optical depth of OD $= 12.7$, deduced from a fit with a saturated Lorentzian distribution (red line). The transmission without atoms (gray line) is close to unity. The residual modulation is reminiscent of the cavity resonances because the resonator is not perfectly overcoupled. (b) Measured (blue line) and calculated spectrum (red line) of the coupled atom-resonator system. In comparison to the empty resonator spectrum (gray line), the central resonance is split and higher-order resonances are shifted outwards—a clear signature of superstrong coupling. The theory prediction relies on $\kappa_{\mathrm{ext}}/2\pi = 0.39$ MHz and $\kappa_0/2\pi = 0.21$ MHz, which are deduced from the empty resonator spectrum, and the collective coupling strength, $g_N/2\pi = 9.2\ \mathrm{MHz} = 1.3 \times \nu_{\mathrm{FSR}}$, which is deduced from the OD measured in (a). The atom-resonator detuning, $\Delta_{\mathrm{at}} = \omega_{\mathrm{at}} - \omega_{\mathrm{res}}$, is left as a free fit parameter which is found to be $\Delta_{\mathrm{at}}/2\pi = 150$ kHz.

operates in the superstrong coupling regime. The slight deviation between theory and measurement can possibly be attributed to the dipole forces exerted by the probe light in the resonator. These have been shown to result in a detuning-dependent atomic density near the nanofiber surface [38]. In the present experiment this then leads to a detuning-dependent collective coupling strength, g_N, which is not included in the model. Given the fact that the atom-resonator detuning is much smaller than collective coupling strength, the single-atom decay rate, and the FSR, we set $\Delta_{\mathrm{at}} = 0$ in what follows. The limited contrast of the split resonance is due to the fact that our system operates in the regime where the atomic linewidth is comparable to the free-spectral range, $\gamma/2\pi = 0.37 \times \nu_{\mathrm{FSR}}$. If higher contrast is required, this can in principle be achieved by proportionally increasing ν_{FSR} and g_N. For example, decreasing the resonator length by a factor of 3 while increasing the atom number by the same factor would increase the contrast of the split resonance by an order of magnitude.

Figure 3(a) shows a series of transmission spectra in dependence of g_N. The latter is set by varying N via the waiting time between switching off the MOT and probing the atom-resonator system. The abscissa values of g_N are deduced from fitting our model to the individual experimental spectra, see [33]. For $g_N/(2\pi\nu_{\mathrm{FSR}}) \gtrsim 1$, a splitting of the central resonance becomes visible and increases with g_N. Moreover, the outer resonances are progressively

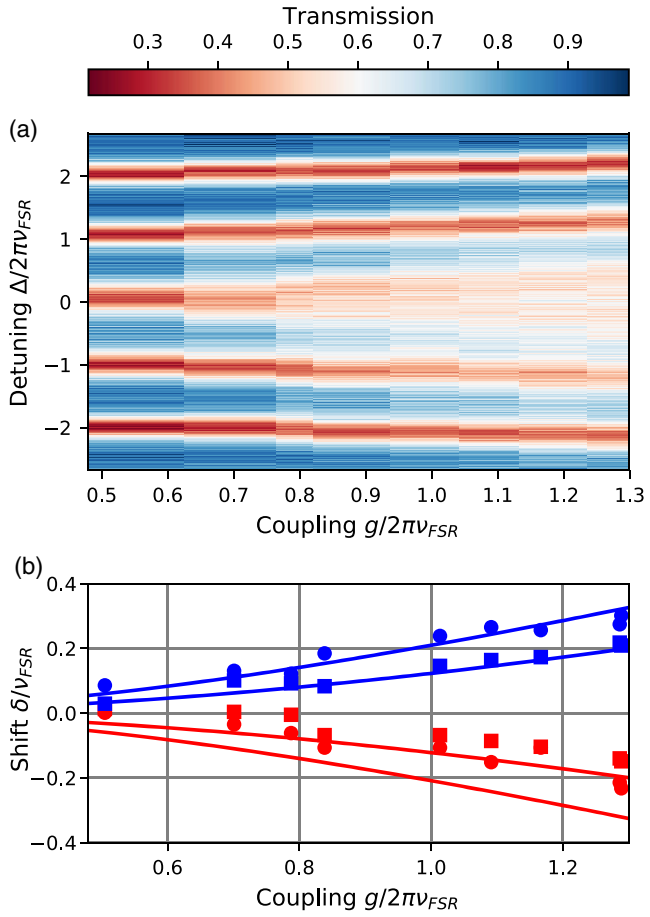

FIG. 3. (a) Transmission of the atom-resonator system with increasing collective coupling strength g_N. The abscissa values of g_N are deduced from fitting the individual spectra. A splitting of the central resonance and an outward shift of the adjacent resonances that increase with g_N are clearly visible, thus highlighting the superstrong nature of strong coupling. (b) Frequency shift of the transmission minima with respect to the empty cavity resonances. The red and blue squares and circles mark the positions of the transmission dips extracted from the experimental spectra. The solid lines give the theoretical prediction for the positions of transmission minima. The circles represent the $\pm$1st-order modes, whose bare-resonator frequency differs by $\pm\nu_{\mathrm{FSR}}$ from the central resonance, and the squares the $\pm$2nd-order modes. As expected, both pairs of modes show a substantial shift on the scale of ν_{FSR}, where the magnitude of the shifts of the $\pm$1st-order modes is larger than for the $\pm$2nd-order modes.

shifted outwards, and become shallower. The maximum coupling found here is $g_N/2\pi = (9.2 \pm 0.07)$ MHz, in good agreement with the independently measured value from Fig. 2(a). Figure 3(b) shows the frequency shift δ of the $\pm$1st-order and the $\pm$2nd-order resonator modes from their original positions in the empty resonator as a function of g_N. Here, the magnitude of the shift of each mode increases with coupling strength: the $\pm$1st-order modes (shown in circles) shift more strongly than the $\pm$2nd-order modes (in squares) which are further detuned from the atomic transition. The solid lines give the theoretical prediction for the positions of the modes. The agreement with the theoretical prediction is very good for the $+$1st- and $+$2nd-order modes. For the $-$1st- and $-$2nd-order modes, the observed shifts are smaller than expected from theory. We attribute this discrepancy to the detuning-dependent coupling strength caused by the dipole forces exerted by the probe light, see above.

In order to measure the number of coupled atoms N we excite the atomic cloud with the MOT laser beams and collect the resonance fluorescence photons that are emitted into the nanofiber-guided mode. For this measurement, the fiber loop is open such that the light is directly guided towards the detector. The information on N is then contained in the second-order (intensity-intensity) correlation function $g^{(2)}(\tau)$. The measurement sequence alternates between a cooling phase (200 μs of magneto-optical trapping) and a 20-μs long fluorescence phase during which the MOT beams are switched into resonance with the atoms. In this setting, the form of $g^{(2)}(\tau)$ depends on the number of emitters contributing to the signal [39]. For a small number of atoms, $g^{(2)}(\tau)$ exhibits antibunching. This is because the intensity correlation function is mainly due to single photons emitted by individual atoms. On the contrary, when many atoms contribute to the signal, $g^{(2)}(\tau)$ exhibits bunching. This stems from two-photon interference of the light emitted into the fiber by pairs of atoms. The transition from bunching to antibunching happens for small atom numbers, which is the regime we placed ourselves in for this calibration measurement [40,41]. Performing this measurement for OD $= 0.06 \pm 0.01$, 0.11 ± 0.02, and 0.20 ± 0.01, determined from independently measured transmission spectra, we obtain the correlation data shown in Fig. 4.

We fit the model from [39] to the correlation data, see Supplemental Material, and find effective numbers of coupled atoms of $N_{\mathrm{eff}} = 2.7 \pm 0.3$, 4.3 ± 0.3, and 9.5 ± 0.5. For low OD, the theoretical prediction agrees well with the data. However, for OD ≥ 0.2, it begins to deviate because reabsorption of the fiber-guided fluorescence by the atoms becomes significant and is not included in the model. From N_{eff} and the respective ODs, we deduce an average optical depth per atom of $\mathrm{OD}_1 = 0.022 \pm 0.005$. This corresponds to an intrinsic single-atom cooperativity of $C_1 = 0.13$ [33], a value which

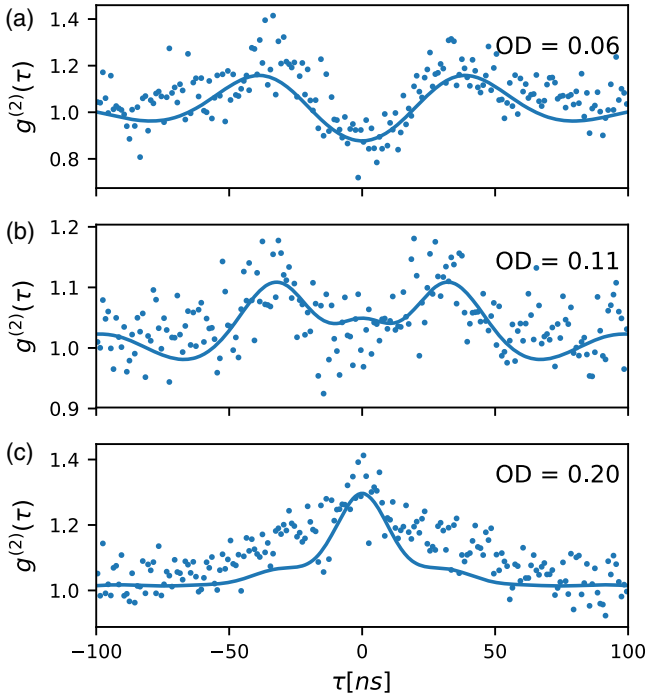

FIG. 4. Second-order correlation measurements taken for three different ODs. Fitting the correlation data yields effective numbers of coupled atoms of 2.7, 4.3, and 9.5, respectively. (a) $g^{(2)}(\tau)$ exhibits antibunching and $g^{(2)}(0)$ drops below 1. (b) With on average 4.3 atoms contributing to the signal, $g^{(2)}(\tau)$ also shows antibunching, but $g^{(2)}(0)$ does not drop below 1. Finally, in (c) $g^{(2)}(\tau)$ exhibits a clear bunching signal, owing to the fact that far more than one atom contributes to the measured signal. From these measurements we deduce an OD per atom of 0.022.

remains substantial despite the very long resonator. Using OD_1, we can now convert any measured total OD into the effective number of coupled atoms. In particular, the threshold to SSC is reached with as little as $N_{\mathrm{eff}} = 294 \pm 34$ atoms and the largest collective coupling of $g_N/2\pi = 1.3 \times \nu_{\mathrm{FSR}}$ presented in Fig. 3 requires only $N_{\mathrm{eff}} = 645 \pm 109$ atoms.

The experimental realization of superstrong coupling for only 200 atoms sets the stage for devising novel applications and for the scientific exploration of cavity QED in an entirely new regime. For example, the expected non-Markovian dynamics of our experimental system is challenging theoretically and uncharted experimentally. In this context, pulsed revivals of the atomic inversion on the time scale of the round-trip time of the resonator, rather than sinusoidal vacuum Rabi oscillations, have been predicted [42]. Moreover, the interaction of different cavity modes that occurs under the condition of SSC, in conjunction with the substantial single-atom cooperativity, should enable resonator-enhanced wave mixing of fields containing only a few photons each. Finally, our system may also pave the way towards the implementation of

quantum annealing algorithms using atoms [43] or photons [44] as carriers of information.

We thank Helmut Ritsch, Stefan Rotter, and Matthias Sonnleitner for helpful discussions. Financial support from the European Research Council (CoG NanoQuaNt) and the Austrian Science Fund (FWF, CoQuS Project No. W1210-N16 and NanoFiRe Grant Project No. P31115) is gratefully acknowledged.

*juergen.volz@hu-berlin.de

[1] H. J. Kimble, Phys. Scr. **T76**, 127 (1998).
[2] A. Reiserer and G. Rempe, Rev. Mod. Phys. **87**, 1379 (2015).
[3] T. Wilk, S. C. Webster, A. Kuhn, and G. Rempe, Science **317**, 488 (2007).
[4] A. D. Boozer, A. Boca, R. Miller, T. E. Northup, and H. J. Kimble, Phys. Rev. Lett. **98**, 193601 (2007).
[5] A. Stute, B. Casabone, B. Brandstatter, K. Friebe, T. E. Northup, and R. Blatt, Nat. Photonics **7**, 219 (2013).
[6] J. Volz, R. Gehr, G. Dubois, J. Estève, and J. Reichel, Nature (London) **475**, 210 (2011).
[7] T. G. Tiecke, J. D. Thompson, N. P. de Leon, L. R. Liu, V. Vuletić, and M. D. Lukin, Nature (London) **508**, 241 (2014).
[8] B. Hacker, S. Welte, G. Rempe, and S. Ritter, Nature (London) **536**, 193 (2016).
[9] M. Scheucher, A. Hilico, E. Will, J. Volz, and A. Rauschenbeutel, Science **354**, 1577 (2016).
[10] Y. Colombe, T. Steinmetz, G. Dubois, F. Linke, D. Hunger, and J. Reichel, Nature (London) **450**, 272 (2007).
[11] W. Chen, K. M. Beck, R. Bücker, M. Gullans, M. D. Lukin, H. Tanji-Suzuki, and V. Vuletic, Science **341**, 768 (2013).
[12] I. D. Leroux, M. H. Schleier-Smith, and V. Vuletić, Phys. Rev. Lett. **104**, 073602 (2010).
[13] J. E. Florian Haas, J. Volz, R. Gehr, and J. Reichel, Science **344**, 180 (2014).
[14] M. Hosseini, K. M. Beck, Y. Duan, W. Chen, and V. Vuletić, Phys. Rev. Lett. **116**, 033602 (2016).
[15] K. Baumann, C. Guerlin, F. Brennecke, and T. Esslinger, Nature (London) **464**, 1301 (2010).
[16] H. Ritsch, P. Domokos, F. Brennecke, and T. Esslinger, Rev. Mod. Phys. **85**, 553 (2013).
[17] H. Keßler, J. Klinder, M. Wolke, and A. Hemmerich, New J. Phys. **16**, 053008 (2014).
[18] N. Spethmann, J. Kohler, S. Schreppler, L. Buchmann, and D. M. Stamper-Kurn, Nat. Phys. **12**, 27 (2016).
[19] N. Schine, A. Ryou, A. Gromov, A. Sommer, and J. Simon, Nature (London) **534**, 671 (2016).
[20] K. E. Ballantine, B. L. Lev, and J. Keeling, Phys. Rev. Lett. **118**, 045302 (2017).
[21] N. Jia, N. Schine, A. Georgakopoulos, A. Ryou, L. W. Clark, A. Sommer, and J. Simon, Nat. Phys. **14**, 550 (2018).
[22] A. Wickenbrock, M. Hemmerling, G. R. M. Robb, C. Emary, and F. Renzoni, Phys. Rev. A **87**, 043817 (2013).
[23] M. Brune, F. Schmidt-Kaler, A. Maali, J. Dreyer, E. Hagley, J. M. Raimond, and S. Haroche, Phys. Rev. Lett. **76**, 1800 (1996).
[24] P. Lodahl, S. Mahmoodian, and S. Stobbe, Rev. Mod. Phys. **87**, 347 (2015).
[25] D. Meiser and P. Meystre, Phys. Rev. A **74**, 065801 (2006).
[26] N. M. Sundaresan, Y. Liu, D. Sadri, L. J. Szőcs, D. L. Underwood, M. Malekakhlagh, H. E. Türeci, and A. A. Houck, Phys. Rev. X **5**, 021035 (2015).
[27] B. A. Moores, L. R. Sletten, J. J. Viennot, and K. W. Lehnert, Phys. Rev. Lett. **120**, 227701 (2018).
[28] P. Schneeweiss, S. Zeiger, T. Hoinkes, A. Rauschenbeutel, and J. Volz, Opt. Lett. **42**, 85 (2017).
[29] P. Solano, J. A. Grover, J. E. Hoffman, S. Ravets, F. K. Fatemi, L. A. Orozco, and S. L. Rolston, Adv. At. Mol. Opt. Phys. **66**, 439 (2017).
[30] T. Nieddu, V. Gokhroo, and S. N. Chormaic, J. Opt. **18**, 053001 (2016).
[31] S. Kato and T. Aoki, Phys. Rev. Lett. **115**, 093603 (2015).
[32] S. K. Ruddell, K. E. Webb, I. Herrera, A. S. Parkins, and M. D. Hoogerland, Optica **4**, 576 (2017).
[33] See Supplemental Material at http://link.aps.org/supplemental/10.1103/PhysRevLett.123.243602 for observation of multimode strong coupling of cold atoms to a 30-m long optical resonator, which includes Refs. [34,35].
[34] J.-T. Shen and S. Fan, Phys. Rev. A **79**, 023837 (2009).
[35] E. Vetsch, D. Reitz, G. Sagué, R. Schmidt, S. T. Dawkins, and A. Rauschenbeutel, Phys. Rev. Lett. **104**, 203603 (2010).
[36] T. Hänsch and B. Couillaud, Opt. Commun. **35**, 441 (1980).
[37] A. Libson, N. Brown, A. Buikema, C. C. López, T. Dordevic, M. Heising, and M. Evans, Opt. Express **23**, 3809 (2015).
[38] G. Sagué, E. Vetsch, W. Alt, D. Meschede, and A. Rauschenbeutel, Phys. Rev. Lett. **99**, 163602 (2007).
[39] F. Le Kien and K. Hakuta, Phys. Rev. A **77**, 033826 (2008).
[40] K. P. Nayak, F. Le Kien, M. Morinaga, and K. Hakuta, Phys. Rev. A **79**, 021801(R) (2009).
[41] J. A. Grover, P. Solano, L. A. Orozco, and S. L. Rolston, Phys. Rev. A **92**, 013850 (2015).
[42] D. O. Krimer, M. Liertzer, S. Rotter, and H. E. Türeci, Phys. Rev. A **89**, 033820 (2014).
[43] V. Torggler, S. Krämer, and H. Ritsch, Phys. Rev. A **95**, 032310 (2017).
[44] P. L. McMahon, A. Marandi, Y. Haribara, R. Hamerly, C. Langrock, S. Tamate, T. Inagaki, H. Takesue, S. Utsunomiya, K. Aihara, R. L. Byer, M. M. Fejer, H. Mabuchi, and Y. Yamamoto, Science **354**, 614 (2016).